*Hadi Ebrahim Fathabadi, Mohammad Ghorbani**

Sharif University of Technology, Materials Science and Engineering Department, Tehran, Iran

Scientific paper
ISSN 0351-9465, E-ISSN 2466-2585
https://doi.org/10.5937/zasmat2302134F

Zastita Materijala 64 (2)
134 - 152 (2023)

Investigation of the corrosion inhibition properties of hexamine (HMTA) for mild steel in NaCl solution

ABSTRACT

An effective corrosion inhibitor for steel is Hexamine (HMTA). There have been few studies on its corrosion-inhibiting characteristics, particularly in NaCl solution. The electrochemical characteristics of HMTA performance in NaCl 3.5 wt % solution were examined during this study. Additionally, the properties of the HMTA film on the steel surface was investigated. When tested in NaCl solution, electrochemical results revealed that HMTA is a very efficient corrosion inhibitor for mild steel, with an efficacy of 92% at a concentration of 0.08 M. HMTA exhibited mixed type activity in terms of inhibition, according to the findings. Due to the physical adsorption of HMTA compound, as shown by the XRD results, an organic layer was formed as a strategy for HMTA inhibition. Adsorption of chloride ions as a corrosive factor is reduced by the HMTA films, according to EDS and thermodynamic studies.

Keywords: *Hexamine (HMTA), corrosion inhibition, mild steel, NaCl solution.*

1. INTRODUCTION

Corrosion is a subject of great importance because of its safety and economical related concerns [1,2]. Corrosion inhibitors are chemicals that efficiently slow the corrosion rate of metals and alloys when used in relatively low concentrations [3-5]. Because they adsorb on the surface of the metal by donating electrons, including unpaired electrons or those from aromatic rings in functional groups containing atoms, particularly nitrogen, oxygen, and sulfur, a large number of organic compounds are being employed as corrosion inhibitors [6-8]. Also organic compounds are effective and profitable corrosion inhibitors because of their association with E4 (Efficiency, Economy, Ecology and environmental friendly) [9].

Nitrogen molecules, which create physical or chemical interactions with metal surfaces, are effective inhibitors [10,11]. The character and surface charge of the metal, the charge dispersion in the molecule, the association pattern between the metallic surface and organic compounds, which is determined by the inhibitor's dipole moment, and the organic inhibitor's chemical composition are several variables impacting inhibitor adsorption [12-14].

As hexamine is water-soluble, inexpensive, and possesses four pairs of unshared electrons for donation (HMTA or HMT), its research is of particular importance. In various conditions, hexamine was shown to be an efficient corrosion inhibitor for several metals [15-19]. Figure 1 shows the HMTA chemical structure.

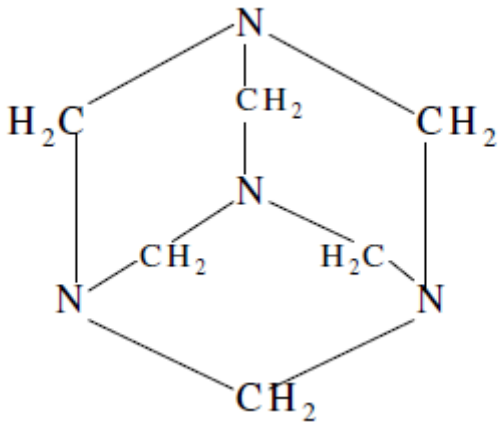

Figure 1. Hexamine (HMTA) chemical structure – $C_6H_{12}N_4$ [20]

Slika 1. Hemijska struktura HMTA - $C_6H_{12}N_4$ [20]

*Corresponding autor: Mohammad Ghorbani
E-mail: ghorbani@sharif.edu
Paper received: 07. 09. 2022.
Paper accepted: 01. 10. 2022.
Paper is available on the website: www.idk.org.rs/journal

Other organic compounds such as plastics, medicines, and rubber additives may be synthesized using HMTA's symmetric tetrahedral cage-like arrangement. When ammonia and formaldehyde are combined, HMTA is produced in the industrial sector. In either the solution or gas phase, the mixture may be formed [21]:

$$4NH_3 + 6CH_2O \rightarrow C_6H_{12}N_4 + 6H_2O \quad (1)$$

Physical and chemical adsorption contribute to the corrosion inhibition of HMTA. Under acidic conditions, HMTA may degrade into formaldehyde and ammonia. Because of the action of van der Waals forces and the presence of formaldehyde, HMTA has a low molecular weight, which allows it to bind physically on metal surfaces. The unpaired electron pair of N atoms and vacant orbits d on the metal surface of HMTA induce its adsorption in the manner of chemical adhesion on the metal surface [22-25]. Regarding carbon steel in a 15 percent hydrochloric acid (HCl) mixture, Liujia et al. tested hexamine as a corrosion inhibitor. In this research, they discovered that hexamine might adsorb on surfaces in both the physical and chemical manner [22]. Hexamine was shown to be an excellent corrosion inhibitor for API 5L X65 in 0.1M HCl, with an optimal concentration of 600 ppm required to achieve a corrosion rate of 0.4 mm/year [26], according to Ogunbadejo et al. Hexamine was investigated by Aribo et al. for its ability to prevent mild steel in 1M HCl from corroding. The findings revealed that the inhibition effectiveness was 86% when the inhibitor concentration was 0.8 g/L [27]. In agreement with the Langmuir isotherm, the findings show that the adsorption was caused by physical reactions. Using HCl 15% solution, Hu et al. evaluated the effects of combining thiourea and hexamine as a corrosion inhibitor for N80. An isothermal analysis of the inhibitor indicated that it adsorbs both chemically and physically, indicating a mixed-type process [18]. Bayol et al. investigated the use of hexamine in acidic mixtures (HCl and H_2SO_4) to limit the corrosion of steel. A physical process called Langmuir adsorption was used to establish that hexamine was a mixed-type inhibitor [19].

There is a combined form of corrosion inhibition of steel using hexamine hydroiodide (HMTA-I) in hydrochloric acid mixtures, according to Mor et al. [28]. Mammalian and aquatic species are generally unaffected by hexamine's presence in the environment. Hexamine, on the other hand, disintegrates into formaldehyde and ammonia when exposed to acidic circumstances or microbial attack. Aquatic species are poisoned by these chemicals [29].

By conducting morphological, electrochemical, and thermodynamically tests, the corrosion prevention characteristics of HMTA for mild steel in 3.5 percent (0.6 M) NaCl mixture, which is a typical salt concentration in sea water (according to ASTM G44-21) and can be used as a solution for corrosion studies of many corrosive agents [30], were evaluated. Numerous studies have examined the corrosion inhibition of HMTA in various acidic conditions, but only a few have looked at this mechanism in NaCl mixture.

2. LABORATORY WORKS

2.1. Samples and solutions preparation

Substrates were made of API 5L steel pipeline Grade B, which had the following composition (in weight percent): C 0.13%, Mn 1.0%, Si 0.22%, Cu 0.1%, Mo 0.01%, P 0.008%, S 0.005%, and Fe equilibrium. To produce a contact surface of 10 mm × 10 mm, the specimens were sliced and covered with a cold-curing epoxy resin. Emery sheets of SiC were used to abrade the surfaces of steel specimens, ranging from 60 to 1200 grit. Before being degreased in ethanol (purity of 99.8 percent), the samples were washed using deionized water. A desiccator was subsequently used to maintain the specimens. Using emery paper of SiC, specimens were pulverized up to 1500 grit and then burnished employing a 1μm diamond suspension. In the next steps, the specimens were washed using deionized water and solubilized in ethanol, and then they were allowed to dry naturally. It was necessary to make a mixture containing 3.5 wt.% NaCl. Various quantities of Hexamine (Merk, Germany, CAS 100-97-0) were introduced to the mixtures with various concentrations (0, 0.01, 0.03, 0.05, 0.08, 0.09 M). Two hours was the amount of time it took for solutions to agitate.

2.2. Electrochemical Studies

A potentiostat/Galvanostat Autolab 302N (Switzerland) coupled with Nova 1.11 software was used to evaluate electrochemical parameters. As a counter electrode, a platinum plate measuring 3 cm × 1 cm was employed. In contrast to a saturated calomel electrode (SCE), potentials were measured. The distance between the working and counter electrodes was 1 cm [31]. To begin, a plot of the open circuit potential (OCP) vs. time was made to understand better how solution stabilization occurs. A potential scanning frequency of 0.1 mV/s and a potential spectrum of -100 mV to +100 mV (vs. OCP) were used to draw the potentiostatic polarization graphs, which were acquired 50 minutes following stabilization in NaCl mixtures. The inhibition effectiveness, IE, is determined by Equation 2 as follows:

$$IE\% = \frac{i^0_{corr} - i_{corr}}{i^0_{corr}} \times 100\% \quad (2)$$

where i^0_{corr} (mA/cm^2) and i_{corr} (mA/cm^2) represent corrosion current densities in the solution, in the absence and presence of inhibitor, respectively.

Varying concentrations (0 to 0.09 M HMTA) and temperatures (293, 303, 313, and 323 K) were used during the polarization experiments. Corrosion current density (i_{corr}), corrosion potential (E_{corr}), anodic Tafel slope (β_a), and cathodic Tafel slope (β_c) were all electrochemical corrosion characteristics derived from polarization graphs. Using an OCP (Open Circuit Potential) with a limited AC voltage of 10 mV and a frequency of 100 Hz to 0.01 Hz, EIS information was also collected on the steel electrode following 50 minutes of soaking in the mixtures. EG&G PRINCETON APPLIED RESEARCH conducted the EIS using Power Suite software.

Equation 3 estimates the inhibition efficiency (IE) [32-34].

$$IE\% = 100 \times (R_p^i - R_p^0) / R_p^i \quad (3)$$

where R_p^i and R_p^0 denote working electrode polarization resistances with and without of HMTA inhibitor, respectively.

2.3. Isotherm of adsorption and thermodynamic aspects

Adsorption isotherms were examined in order to elucidate the adsorption of organic corrosion inhibitors and the metal-surface association. Correlation coefficients (R^2) were utilized to choose the optimal modifications based on the adsorption isotherms analyzed, including Temkin, Freundlich, and Langmuir. The Equation for Temkin, Freundlich and Langmuir adsorption isotherms are as follows:

$$K_{ads}C = exp(-2a\theta) \quad (Temkin) \quad (4)$$

a denotes a variable for the molecular association, θ represents the surface coverage extent, $\mathbf{K_{ads}}$ is the constant of adsorption process balance, and **C** denotes the inhibitor concentration [35].

$$log\,\theta = log\,K_{ads} + \frac{1}{n} log\,C \quad (Freundlich) \quad (5)$$

where **n** represents a constant [36].

$$\frac{C}{\theta} = \frac{1}{K_{ads}} + C \quad (Langmuir) \quad (6)\ [37]$$

2.4. Surface Analysis by SEM, EDS, AFM, XRD Techniques

A study of the metal surface morphology subjected to NaCl solutions containing various amounts of HMTA examined and the impact of HMTA compound adsorption on steel corrosion suppression investigated. Phenom ProX Desktop SEM was used to examine the subjected metal surfaces once submerged for two hours in 3.5 wt.% NaCl mixtures comprising 0, 0.01, 0.03, 0.05 and 0.08 M HMTA. EDS (Energy-dispersive X-ray spectroscopy) evaluation was performed using the FESEM TESCAN MIRA III with a SAMX detector. Following 8 hours of immersion in mixtures containing varying concentrations of HMTA, steel electrodes were subjected to atomic force microscopy (NTEGRA AFM NT – MDT). 450 μm × 50 μm × 2 μm triangular cantilevers were used to hold the AFM silicon tip. The cantilevers had an average spring constant of 0.02 to 0.77 N/m. The scanning process was carried out using a contact model, with a scanning range, rate and resolution of 10 μm × 10 μm, 1Hz, and 256 × 256 pixels, respectively. Cu-K radiation at 40 kV and 40 mA was employed to explore the impacts of inhibitor layers on crystalline phases of steel surface using a scanning angle of 10° to 90° and a 0.026 ° step size in the X-ray diffraction (Diffractometer system XPERT-PRO, 2500 V).

3. RESULTS AND DISCUSSIONS

3.1. Open Circuit Potential (OCP) Results

Figure 2 shows OCP curves as a function of immersion duration for steel electrode in 3.5 wt.% NaCl mixtures with varying concentrations of hexamine (HMTA) (0 to 0.08 M).

The OCP seeks to be more positive when HMTA is added to NaCl mixtures. After 15 minutes of soaking in the blank mixture (0.0 M HMTA), the OCP approaches -0.6 V_{SCE}. When HMTA is added, it causes the OCP graphs to shift in a more positive direction. Because of the creation of protecting coatings and contacts between inhibitor on the steel surface, the stabilization duration increases. OCP is predicted to stabilize within 40 to 50 minutes, depending on the inhibitor dosage. As a result, the period of stabilization is defined as 50 minutes. Due to HMTA's inhibitory actions on steel in NaCl mixtures in which HMTA is immobilized on both cathodic and anodic regions of the steel, OCP shifts to less negative potentials are caused by increasing HMTA concentrations. Steel surface anodic processes take longer than expected, resulting in a shift in the OCP to more negative values [38]. The minor change in OCP due to inhibitor addition (up to roughly 60 mV) shows the combined behavioral inhibition of HMTA, as the VSCE changes from -0.6 for the blank mixture to -0.54 V_{SCE} for 0.08 M concentration. Figure 3 depicts the relationship between the provided DC potential and the capacity of the double layer. HMTA was used in a 3.5 wt.% NaCl mixture with and without varying concentrations. As demonstrated in Table 1, the uncontrolled and inhibited solutions of NaCl have E_{PZC} and E_{OCP} levels for mild steel, respectively.

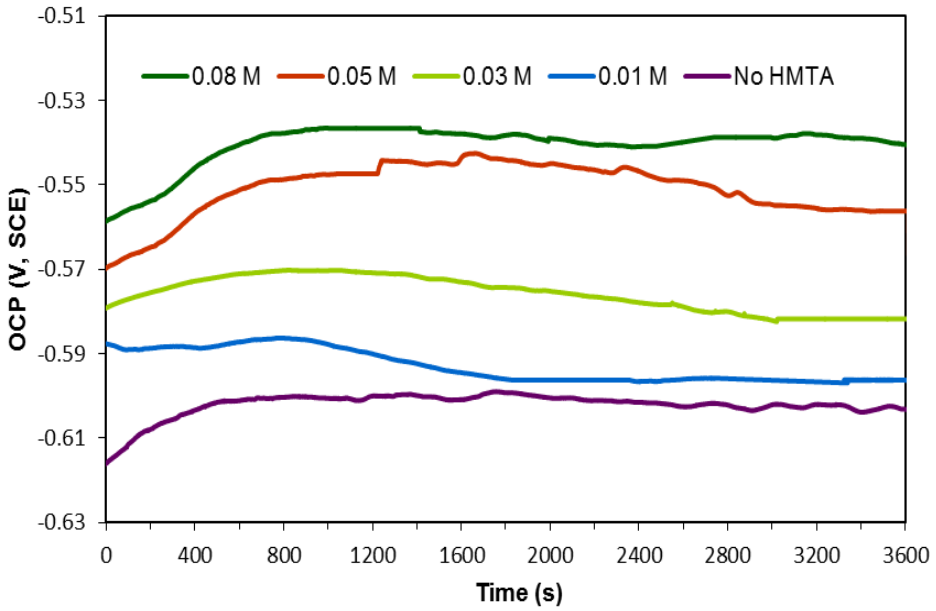

Figure 2. OCP - Open circuit potential of mild steel following 3600s immersion at 293 K in a 3.5 wt.% NaCl mixture containing various concentrations of HMTA (0 to 0.08 M)

Slika 2. OCP - Potencijal otvorenog kola mekog čelika nakon potapanja od 3600s na 293 K u mešavini NaCl od 3,5 tež.% koja sadrži različite koncentracije HMTA (0 do 0,08 M)

The mild steel surface charge at the OCP may be determined from Equation 7 as follows:

$$E_r = E_{OCP} - E_{PZC} \qquad (7)$$

where E_r denotes Antropor's " illustrative " corrosion potential [39].

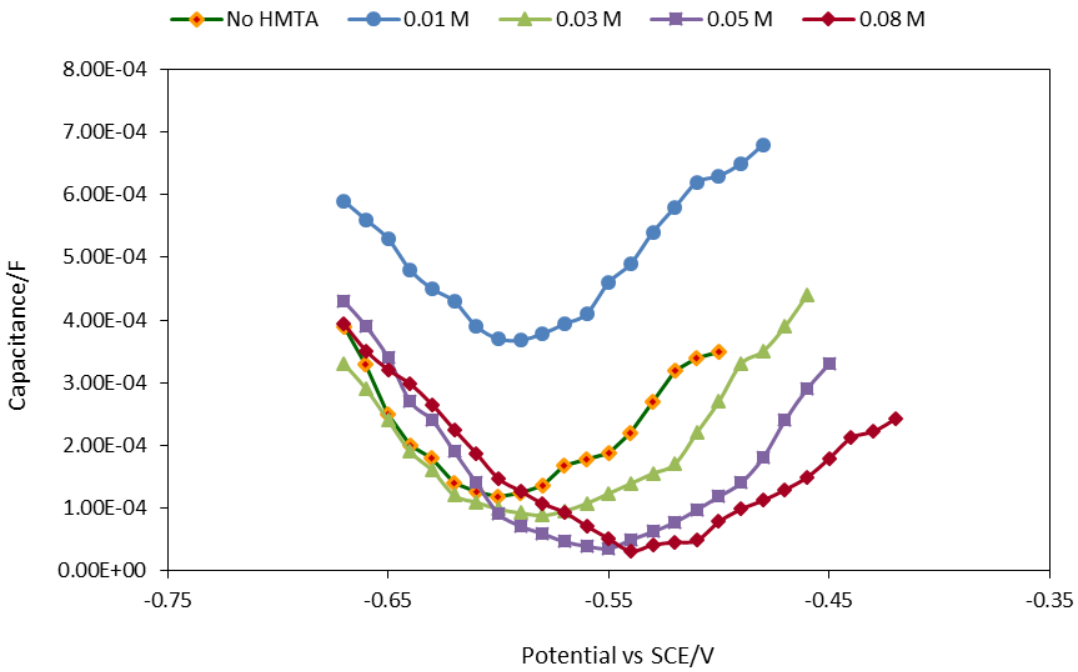

Figure 3. Graph of different capacitance versus supplied electrode potential in 3.5 wt.% NaCl mixture with and without different HMTA concentrations

Slika 3. Grafik različite kapacitivnosti u odnosu na dovedeni potencijal elektrode u 3,5 tež.% smeše NaCl sa i bez različitih koncentracija HMTA

Table 1. Surplus charge on the mild steel electrode in 3.5 wt.% NaCl solution in the absence and presence of different concentrations of HMTA

Tabela 1. Višak naelektrisanja na elektrodi od mekog čelika u 3,5 tež.% rastvora NaCl u odsustvu i prisustvu različitih koncentracija HMTA

Medium	$-E_{OCP}$ (mV)	$-E_{PZC}$ (mV)	Excess Charge
3.5 wt.% NaCl	0.601	0.614	0.013
3.5 wt.% NaCl+0.01 M HMTA	0.596	0.619	0.023
3.5 wt.% NaCl+0.03 M HMTA	0.581	0.625	0.044
3.5 wt.% NaCl+0.05 M HMTA	0.556	0.630	0.074
3.5 wt.% NaCl+0.08 M HMTA	0.539	0.642	0.103

The examination zone from the solution to the metal surface may be achieved by reducing the frequency of the EIS signal when estimating resistance or electrical properties of a system; for example, approaching the evaluation area to the metal surface reduces the frequency. The region of the solution metal interface will be related to the resistance determined at 100-hertz frequency as a result of this. With and without an inhibitor, the mild steel surface charge at OCP was shown to be positive concerning PZC in a 3.5 wt% NaCl mixture [40].

Because mild steel has a positive charge due to anodic degradation, Cl^- ions must first be bound to the metal surface. HMTA molecules in the protonated form (HMTA (H^+)) may be present in HMTA-containing fluids under these circumstances. Because of electrostatic desorption, inhibitor compound possessing positive charges have a tough challenge approaching a positively charged metal surface. There are Cl^- ion bridges that link protonated organic cations to the positively charged metal surface, allowing these molecules to adsorb on the metal surface [41,42].

An inhibitor is more readily adsorbed on the steel surface when chloride ions possess a lower degree of hydration and only adsorb on the metal surface, resulting in an excessive negative charge in the solution phase. Aside from that, Cl^- ions are in direct struggle with HMTA compound for attachment to the metal substrate. The higher the concentration and deposition of HMTA compound, the more positive charges are generated on the metal surface. It is necessary to remember that OH^- ions are generated in cathodic processes from oxygen and water reduction as follows:

$$2H_2O + 2e \rightarrow H_2 + 2OH^-$$

$$O_2 + 2H_2O + 4e \rightarrow 4OH^-$$

The above reactions also can stimulate the adsorption of protonated HMTA compound on the cathodic places. The adsorption of HMTA on accessible sites may occur on the other edge in parallel with physical adsorption, through donor receiver interactions between the π electrons of N atoms of the HMTA and the unoccupied d orbitals of iron when such interactions are feasible. Following roughly 50 minutes, the metal surface potential has stability.

3.2. Corrosion Inhibition Study by Polarization

3.2.1. Inhibitor concentration effect

Polarization graphs for mild steel in 3.5 wt.% NaCl mixture at various HMTA levels (0 to 0.08 M) is shown in Figure 4. As predicted, adding HMTA to the mixture increases the corrosion potential (E_{corr}).

Table 2. Electrochemical corrosion variables determined by polarization experiments of mild steel in a 3.5 wt.% NaCl mixture containing varying amounts of HMTA (0 to 0.09 M)

Tabela 2. Promenljive elektrohemijske korozije određene eksperimentima polarizacije mekog čelika u smeši od 3,5 tež.% NaCl koja sadrži različite količine HMTA (0 do 0,09 M)

Concentration (M)	E_{corr}, (SCE)	i_{corr}, μA/cm^2	β_a, Vdec^{-1}	β_c, Vdec^{-1}	IE (%)
Blank	-0.6023	10.0012	0.0112	0.0121	---
0.01	-0.5923	5.2211	0.0113	0.0122	47.6022
0.03	-0.5814	2.8213	0.0114	0.0121	72.1431
0.05	-0.5609	1.4121	0.0114	0.0123	86.1112
0.08	-0.5421	0.8120	0.0113	0.0122	91.9835
0.09	-0.5432	0.8024	0.0112	0.0121	92.0012

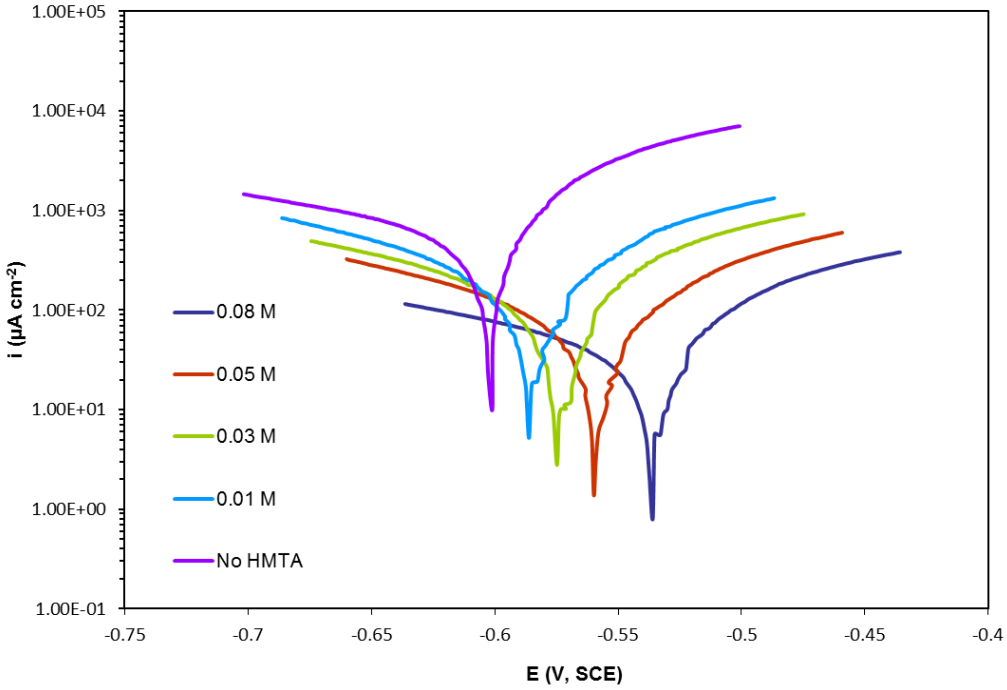

Figure 4. Polarization graphs for mild steel at 293 K in 3.5 wt.% NaCl mixture containing varying concentrations of HMTA (0 to 0.08 M)

Slika 4. Grafici polarizacije za meki čelik na 293 K u 3,5 tež.% smeše NaCl koja sadrži različite koncentracije HMTA (0 do 0,08 M)

Anodic and cathodic graphs both shift to decrease current densities when HMTA quantity is increased. At a constant potential, the inhibitory impact of HMTA on anodic processes is more apparent. Although the anodic and cathodic processes are reduced by HMTA, its influence is more noticeable on anodic reactions because of HMTA's complex nature. Tafel polarization was used to get the electrochemical corrosion data shown in Table 2.

These values included the corrosion current density (i_{corr}), the effectiveness of inhibition (IE%), the inclinations of the anodic and cathodic branches (β_a, β_c), and the effectiveness of inhibition (IE%) as a proportion of HMTA content. It is possible to deduce, based on the data that revealed reduced rates of corrosion processes that the frequency of corrosion current drops significantly with increasing the content of HMTA in NaCl mixture. OCP graphs are consistent with E_{corr} increases caused by the introduction of HMTA. It is confirmed that HMTA has mixed performance when the E_{corr} deflections are less than 85 mV (in this case, 63 mV) [43, 44]. Also discovered is that the slopes of the graphs (β_c and β_a) were altered with the presence of the inhibitor, resulting in some larger fluctuations in the anodic branches (β_a) when the inhibitor is introduced [45].

Increased HMTA concentration results in an increase in the percentage of inhibition, IE%. At room temperature (293 K), the effectiveness of inhibition is 92% whenever the HMTA concentration is 0.08 M. With increasing amounts of HMTA, no significant changes in corrosion rate or inhibitor efficacy were observed, resulting in corrosion suppression effectiveness for 0.09 M HMTA remaining at 92%. For mild steel in NaCl mixture, HMTA has been shown to be a good corrosion inhibitor. Due to the fulfillment of the protective layer deposition on the steel surface, the introduction of more HMTA (above 0.08 M) results in a reasonably durable i_{corr}. Four nitrogen atoms are found in hexamine, including six groups of CH_2. Since electrons may readily be ordered in the ring between the three nitrogen atoms, it's believed to be an efficient inhibitor. The lone pair of electrons in the nitrogen atom may interact with the positively charged metal surface to provide the inhibitory effect. It is also possible that the presence of six groups of methylene contributes to a rise in electron abundance at the nitrogen atom and an elevation in basic strength of HMTA via the inductive action of the compound, which enhances adhesion to metal surfaces. This results in a rise in the inhibitory performance value [20].

Mild steel anodic interactions in NaCl mixtures are caused by Fe ions dissolving, while cathodic processes are mostly connected to oxygen and water reduction.

By replacing the adsorbed water with the organic inhibitors, the HMTA binds to the metal surface [46,47]:

$$Inh_{sol} + xH_2O_{ads} \rightarrow Inh_{ads} + xH_2O_{sol}$$

A Fe-inhibitor combination will be formed on the metal surface when bound HMTA compound come into contact with dissolved Fe^{2+} ions in the solution:

$$Fe \rightarrow Fe^{2+} + 2e^{-}$$

$$Fe^{2+} + Inh_{ads} \rightarrow [Fe - Inh_{ads}]^{2+}_{ads}$$

The corrosive species and the organic inhibitor are engaged in a battle [26]. As a result of the greater number of 'N' atoms and larger macromolecular size of hexamine, it may have encompassed practically all of the metal surface active sites. By inhibiting cathodic and anodic sites with an adhesive layer, a protecting insoluble layer is formed, resulting in an inhibitory action strategy [48]. The substantial electric field intensity provides adequate driving power for the movement of Cl^- ions from solution to film at anodic locations. Additionally, oxygen diffusion occurs. It is conceivable to see the dissolving of Fe into Fe^{2+} along the axes of anodic polarization, and this process may be followed by corrosion and the transport of Fe^{2+} from the plane of external Helmholtz to the bulk mixture. The slopes of the anodic polarization lines altered when the inhibitors were added, indicating that the inhibitors affected the velocity of steel disintegration to the NaCl pure solution. Relative to the purified mixture of NaCl, cathodic corrosion density increases by adding inhibitors, which indicates that the inhibitor may slow down the cathodic process. An additional energy barrier will be created for Cl^- diffusion due to adsorption of the inhibitor on the steel surface since the active sites are covered by the film of adsorbed inhibitor. Furthermore, the layer has the potential to reduce oxygen transport. The cathodic corrosion rate is slowed down as a result of these variables [18]. In other words, the creation and persistence of a protective and impenetrable coating on the metal surface are thought to be responsible for the corrosion inhibitor process. Furthermore, adsorption blocks both cathodic and anodic sites, contributing to the inhibitory effect.

3.2.2. Temperature effect

It was found that mild steel corrosion was affected by several temperatures (293, 303, 313, and 323 K) and varying concentrations of HMTA in 3.5 wt.% NaCl mixture. Figure 5 shows the findings of the polarization study demonstrating the influence of temperature on corrosion inhibition.

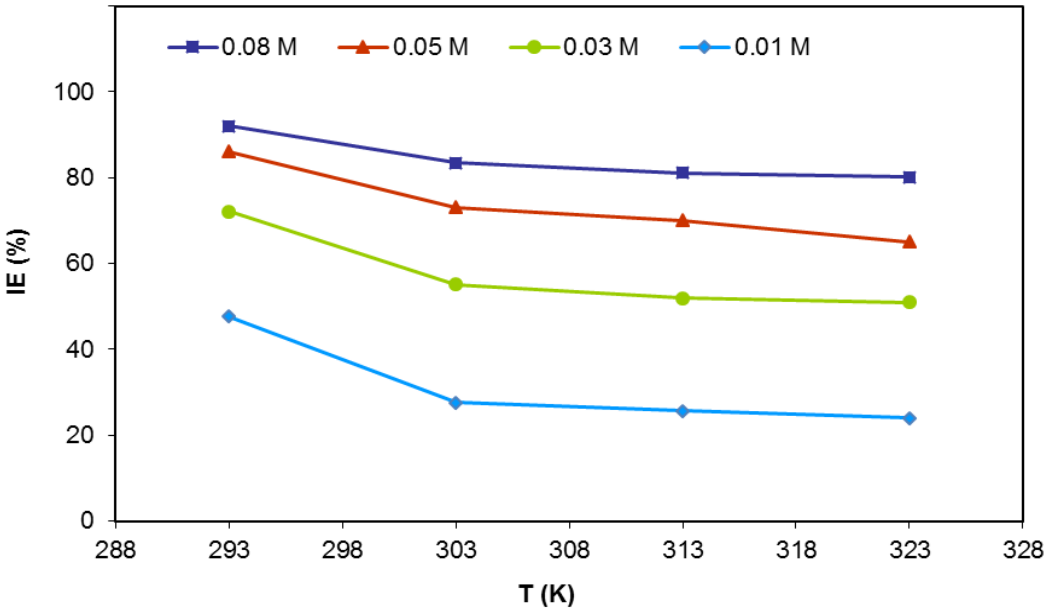

Figure 5. Impact of temperature on the inhibitory efficiency of HMTA on mild steel when different amounts (0.01 to 0.08 M) of HMTA in 3.5 wt.% NaCl mixture is used at varying temperatures (293, 303, 313, and 323 K)

Slika 5. Uticaj temperature na inhibitornu efikasnost HMTA na meki čelik kada se koriste različite količine (0,01 do 0,08 M) HMTA u 3,5 tež.% smeše NaCl pri različitim temperaturama (293, 303, 313 i 323 K)

Table 3 lists the temperature and IE percent at which different HMTA concentrations occur.

Table 3. Corrosion inhibition effectiveness for mild steel in a 3.5 wt.% NaCl mixture with varying HMTA concentrations (0.01 to 0.08 M) at varied temperatures (293, 303, 313 and 323 K)

Tabela 3. Efikasnost inhibicije korozije za meki čelik u smeši od 3,5 tež.% NaCl sa različitim koncentracijama HMTA (0,01 do 0,08 M) na različitim temperaturama (293, 303, 313 i 323 K)

Temperature (K)	IE %			
	0.01 M HMTA	0.03 M HMTA	0.05 M HMTA	0.08 M HMTA
293	47.6	72.1	86.1	92.0
303	27.6	55.1	73.1	83.5
313	25.6	51.9	70.1	81.1
323	24.0	50.9	65.1	80.1

Corrosion inhibition efficacy gradually decreases with increasing temperature, reaching 80% at 323 K for 0.08 M HMTA, as predicted. Increased mild steel dissolving and partial desorption of the HMTA layer from the metal surface contribute to a decrease in inhibitory effectiveness as the temperature rises. This implies that when the temperature rises, the chemical reaction speeds up, the water's viscosity decreases, increasing the unpredictable circulation and diffusion of HMTA. Additionally, this will allow for greater mobility of reagents on the metal surface and, therefore, greater adsorption of HMTA from the metal surface [49]. Also, it is predicted that the efficiencies would rise owing to improved adsorption at temperatures lower than 293 K.

At higher temperatures, the discovered association between IE% and temperature demonstrates HMTA's effectiveness as an inhibitor. At higher temperatures, it is probable that some adsorbed HMTA may be repelled from the surface of the metal, which will result in a decrease in the efficacy of inhibition as well. As a result of this performance, it may be concluded that the HMTA was mostly deposited physically onto the metal surface [20].

3.3. Thermodynamic parameters and adsorption Isotherm

When it comes to matching the data, all three isotherms of adsorption are appropriate, including Temkin, Freundlich, and Langmuir. However, the isotherm of Langmuir provides the greatest match.

Figure 6 depicts the relationship between C/θ and C (0.01 to 0.08 M) at various temperatures (293-323 K). The Langmuir isotherm for HMTA adsorption is supported by information from tests and linear diagrams at different temperatures.

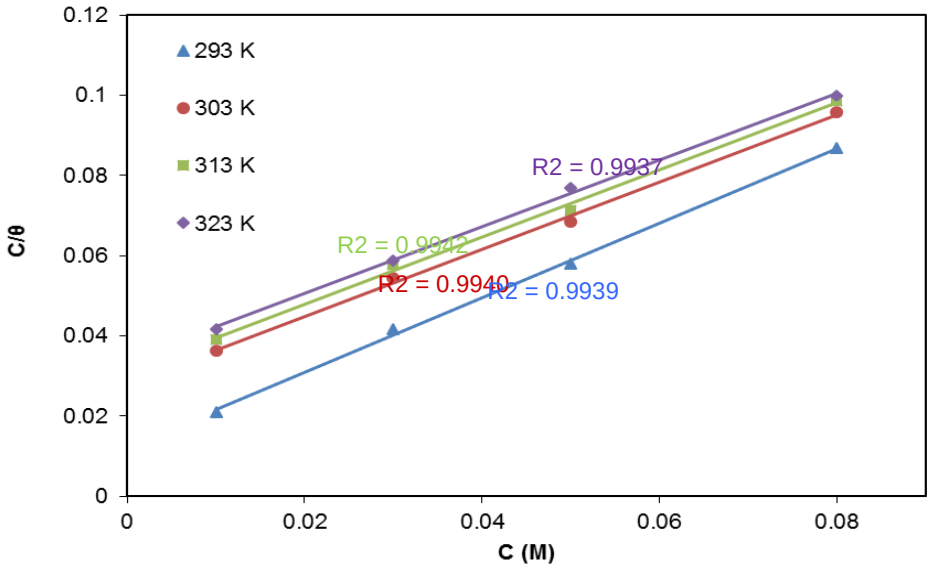

Figure 6. Langmuir adsorption isotherm graphs for steel specimens in 3.5 wt.% NaCl containing varying concentrations of HMTA (0.01 to 0.08 M) at varying temperatures (293, 303, 313 and 323 K)

Slika 6. Langmuir-ovi grafikoni izoterme adsorpcije za čelične uzorke u 3,5 tež.% NaCl koji sadrže različite koncentracije HMTA (0,01 do 0,08 M) na različitim temperaturama (293, 303, 313 i 323 K)

The interaction of reciprocal adsorption and repulsion of polar nitrogen atoms in HMTA was shown by this adsorption isotherm [50]. Table 4 lists the adsorption components obtained from the diagrams.

Table 4. Langmuir adsorption characteristics of mild steel in 3.5 wt.% NaCl mixture containing varying amounts of HMTA (0.01 to 0.08 M) at different temperatures (293, 303, 313, and 323 K)

Tabela 4. Langmuir-ove adsorpcione karakteristike mekog čelika u 3,5 tež.% smeša NaCl koja sadrži različite količine HMTA (0,01 do 0,08 M) na različitim temperaturama (293, 303, 313 i 323 K)

Isotherm (K)	Intercept	Slope	R^2	K_{ads} (M^{-1})
293	0.01	0.93	0.99	81.3
303	0.03	0.84	0.99	35.7
313	0.03	0.84	0.99	32.2
323	0.03	0.83	0.99	29.5

Generally, the larger the K_{ads} acquired from intercepts, the greater the inhibition efficacy of an inhibitor [51]. This is due to its stronger adsorption to the surface of the metal. When the temperature rises, part of the attached inhibitors begins to desorb from the metal surface, giving K_{ads} a temperature-dependent feature. Adsorption of HMTA on the metal surface follows Langmuir's adsorption isotherm, as seen by the proximity of the linear correlation coefficients (R^2) to 1. Langmuir adsorption isotherms have slopes close to 1, indicating a less than ideal isotherm. Unsaturated nuclei on a metal surface may interact with adsorbent inhibitor compounds to cause the divergence from 1 [52].

The heat of adsorption (ΔH_{ads}) can be determined using Van't Hoff Equation 8 [53]:

$$ln\, K_{ads} = \frac{-\Delta H_{ads}}{RT} + D \qquad (8)$$

where D denotes the integration constant, T is the absolute temperature (K) and R is the gas constant (8.314 J K^{-1} mol^{-1}). Figure 7 indicates the linear graph of ln K versus 1000/T (R^2 is 0.87).

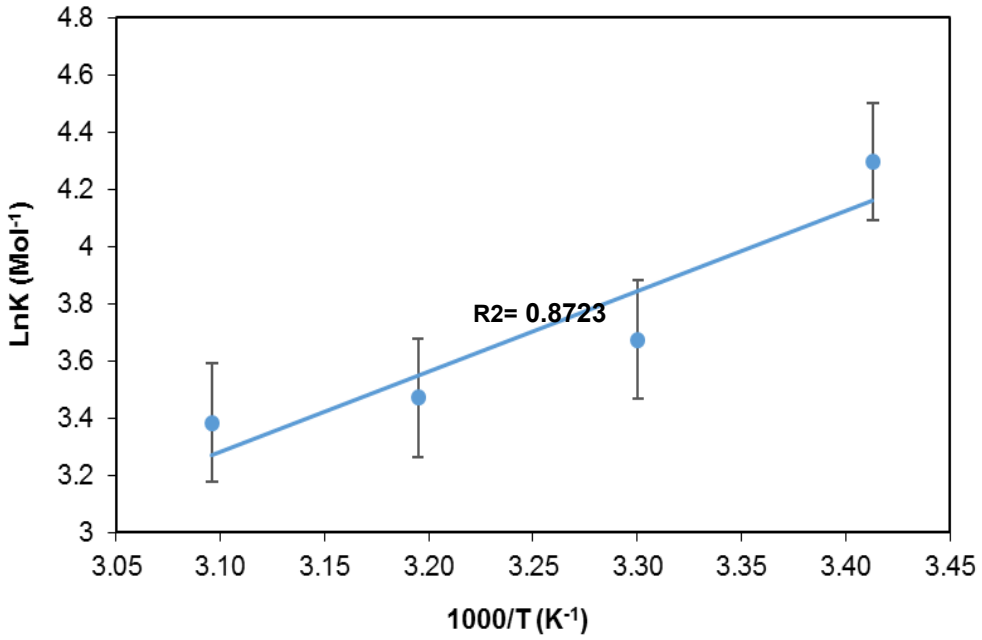

Figure 7. Correlations between the values of $lnK_{ads}(M^{-1})$ and 1000/T(K) of an HMTA inhibitor in a 3.5 wt.% sodium chloride mixture

Slika 7. Korelacije između vrednosti $lnK_{ads}(M^{-1})$ i 1000/T(K) inhibitora HMTA u mešavini natrijum hlorida od 3,5 %tež.

ΔH^0_{ads} can be acquired from the slope ($-\Delta H^0_{ads}/R$) as adsorption processes constant ($kJmol^{-1}$). In the experimental settings, the heat of adsorption may be frequently considered the standard adsorption heat (ΔH^0_{ads}) [51].

Standard adsorption free energy (ΔG^0_{ads}) could be determined using the following Equation 9**:**

$$K = \frac{1}{55} exp(\frac{-\Delta G^0_{ads}}{RT}) \qquad (9)$$

55 denotes the water molar concentration [54-56]. The standard entropy of adsorption (ΔS^0_{ads}) can be determined using Equation 10 as follows:

$$\Delta S^0_{ads} = \frac{\Delta H^0_{ads} - \Delta G^0_{ads}}{T} \quad (10)$$

Table 5 shows the thermodynamic characteristics of the HMTA adsorption isotherms.

Table 5. Thermodynamic parameters for the isotherm of adsorption of HMTA on a mild steel sheet in NaCl mixture

Tabela 5. Termodinamički parametri za izotermu adsorpcije HMTA na meki čelični lim u smeši NaCl

Temperature (K)	ΔG^0_{ads} (kJmol^{-1})	ΔH^0_{ads} (kJmol^{-1})	ΔS^0_{ads} (Jmol^{-1})
293	-20.50	-25.6	-20.58
303	-19.12	-24.4	-19.21
313	-19.49	-24.9	-19.57
323	-19.87	-25.5	-19.95

Exothermic inhibitor adsorption is shown by negative ΔH^0_{ads} values [57]. Adsorption occurs spontaneously, as shown by the negative sign on ΔG^0_{ads} values. A negative ΔG^0_{ads} sign indicates that spontaneous processes liberate free energy as they continue [51].

An increase in metal surface temperature might prompt a few adsorbed inhibitor compounds to be desorbed through exothermic processes. As a result, inhibition may become less effective. That graph in Figure 5 depicts the percentage of IE as a function of temperature. Adsorption processes that have a ΔG^0_{ads} value of -20 kJmol^{-1} or less are carried out by electrostatic reactions between the charged metal layer and charged inhibitors (physisorption), whereas those with a ΔG^0_{ads} value of -40 kJmol^{-1} or more are carried out by electron transition or sharing between the metal layer and the inhibitors for the formation of a chemical linkage (chemisorption) [58,59]. Table 5 shows that ΔG^0_{ads} is roughly -20 kJ mol^{-1}, demonstrating that the character of adsorption is managed by electrostatic relations.

Table 5 shows a negative value for ΔS^0_{ads}, demonstrating the consistency of inhibitors deposited on mild steel surfaces [60]. Adsorption of inhibitors onto steel surfaces may be possible prior to inhibitors being dissolved in the bulk mixture (they were chaotic). However, because of a reduction in entropy, as the adsorption process progressed, molecules of inhibitor were regularly adsorbed onto the steel surface. Due to the fact that adsorption is an exothermic process, it must be accompanied by an increase in entropy, according to thermodynamic considerations as well [61].

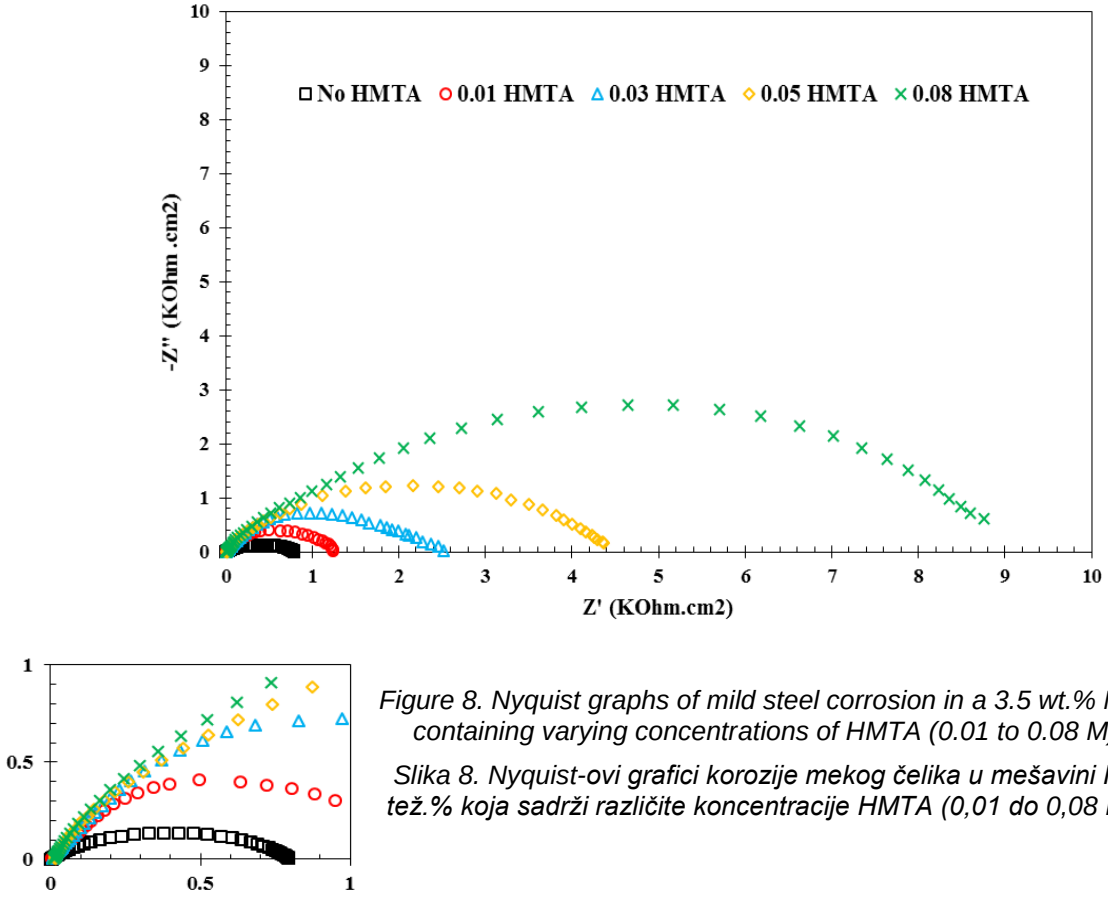

Figure 8. Nyquist graphs of mild steel corrosion in a 3.5 wt.% NaCl mixture containing varying concentrations of HMTA (0.01 to 0.08 M) at 293 K

Slika 8. Nyquist-ovi grafici korozije mekog čelika u mešavini NaCl od 3,5 tež.% koja sadrži različite koncentracije HMTA (0,01 do 0,08 M) na 293 K

3.4. Corrosion inhibition study by EIS

At the electrolyte solution/metal interface generated by inhibitors introduction, EIS (Electrochemical impedance spectroscopy) may be employyed to examine capacitance and resistance layer performance. After 2 hours of immersion in NaCl mixtures containing HMTA concentrations ranging from 0 to 0.08 M, mild steel substrates in the presence of 3.5 wt% NaCl were subjected to EIS in order to evaluate the corrosion inhibition of HMTA.

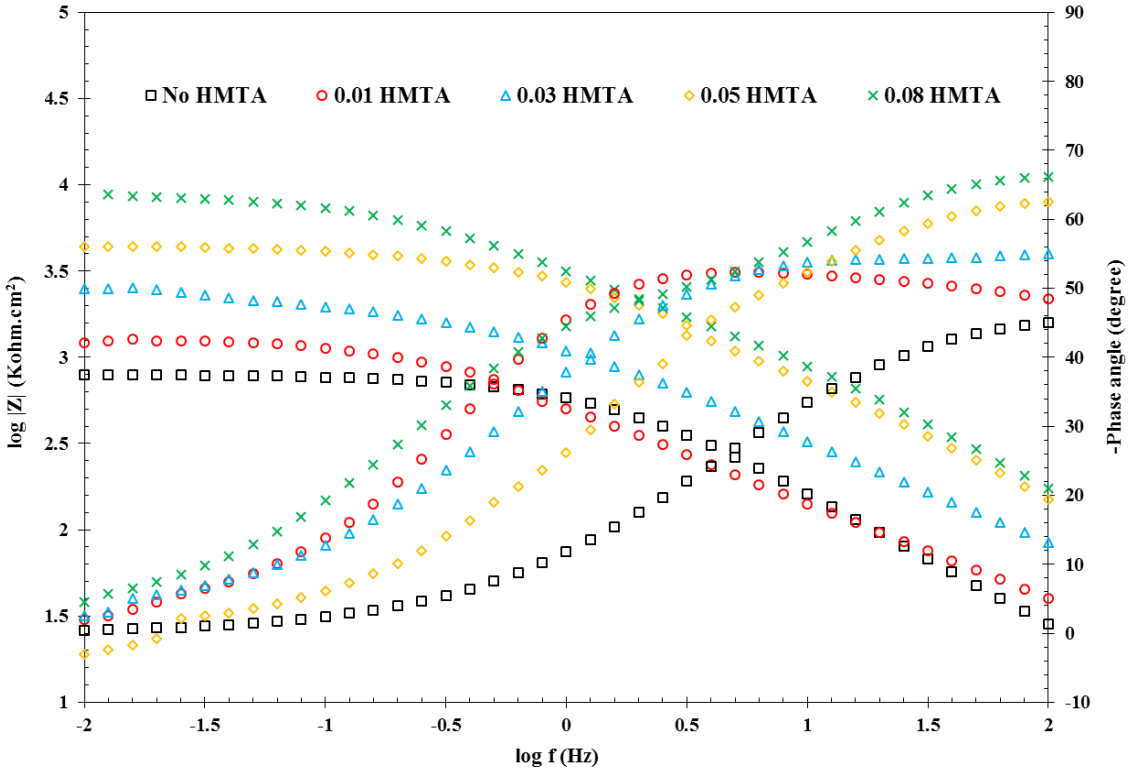

Figure 9. Bode graphs for steel corrosion in 3.5 wt.% NaCl mixture containing varying concentrations of HMTA (0.01 to 0.08 M) at 293 K.

Slika 9. Bode-ovi grafici za koroziju čelika u 3,5 tež.% smeše NaCl koja sadrži različite koncentracije HMTA (0,01 do 0,08 M) na 293 K

In a 3.5 wt.% NaCl mixture containing varying concentrations of HMTA, the Bode and Nyquist graphs for mild steel are shown in Figures 8 and 9.

Regarding resistance to corrosion, the Nyquist diagram's semicircle diameter may be used as an indication. As seen in Figure 8, increasing the inhibitor quantity enhanced the radius of the Nyquist semicircles, indicating that the water droplets bonded on the mild steel surface were substituted by HMTA molecules solubilized in the mixture. Activation, instead of diffusion, controls the corrosion mechanism, as shown by the Nyquist diagram semicircle structure during each experiment

There is only a one-time constant mechanism, as shown by the depressed semicircle in the initial quadrant of the Nyquist graphs. In addition, the "dispersion effect," which is often caused by the roughness and other inhomogeneities of mild steel surfaces, is linked to the depressed capacitive circuits [62, 63].

The entire corrosion resistance of the system may be seen in the lower frequencies absolute resistance of the Bode graphs (Figure 9). Following the trend seen in Figure 8, a rise in the HMTA content leads to an elevation in the absolute resistance at a lower frequency, which is related to the building a protective film of the adsorbed inhibitor on the steel's layer.

To inhibit charge transport from the steel surface, a protective layer was formed, and corrosion was greatly reduced.

Another proof of the protective film generated on the submerged steel surface when HMTA is present is larger positive phase angles at higher inhibitor concentrations when using the maximum frequency.

A well-known approach for interpreting EIS data is electrochemical reaction modeling using equivalent circuits [64,65]. Figure 10 depicts the appropriate comparable circuits in both scenarios.

The resistivity of the solution, charge transfer, and generated film on the steel surface are all shown in Figure 10 by R_s, R_{ct}, and R_f, respectively. C_f and C_{dl} are capacitances of produced film and double layer, correspondingly, in these circuits. Table 6 lists the electrochemical simulation variables [66].

When inhibitor concentrations are increased, substrates exhibiting higher R_{ct} and R_f values will be suppressed, as indicated in Table 6. The specimen containing 0.08 M HMTA had the highest overall resistance

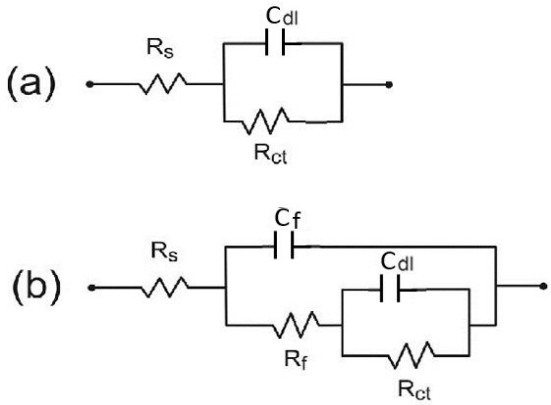

Figure 10. Equivalent circuit model for EIS studies a) with HMTA b) in without HMTA

Slika 10. Model ekvivalentnog kola za EIS studije a) sa HMTA b) u bez HMTA

Table 6. Electrochemical simulation findings for EIS empirical information using appropriate comparable circuits

Tabela 6. Nalazi elektrohemijske simulacije za EIS empirijske informacije korišćenjem odgovarajućih uporedivih kola

Concentration HMTA (M)	R_s ($K\Omega cm^2$)	R_f ($K\Omega cm^2$)	C_f ($\mu F.cm^2$)	R_{ct} ($K\Omega\ cm^2$)	C_{dl} ($\mu F.cm^2$)	R_p ($K\Omega\ cm^2$)	I.E. (%)
0	0.003	0	-	0.74	117.30	0.74	-
0.01	0.005	0.45	329.68	0.92	367.89	1.37	46.1
0.03	0.008	2.52	141.66	0.061	88.23	2.58	71.3
0.05	0.017	4.37	53.80	0.34	34.49	4.7	84.3
0.08	0.018	8.76	50.58	0.74	32.67	9.5	92.2

As shown in Table 6, the lowering trend of C_{dl} with growing inhibitor concentration may be attributed to the creation of a film on the electrode, which results in a rise in the electrical double layer thickness and a drop in the dielectric constant [67]. In addition, the inhibitor concentration was raised, which resulted in an improvement in inhibition effectiveness. At an inhibitor dose of 0.08 M, the inhibition effectiveness reaches its highest value, 92.2%. Findings from potentiostatic polarization, which show high inhibitory effectiveness, are consistent with the impedance measurements.

3.5. Surface morphology evaluation by SEM

Figure 11 shows diffracted electron scanning electron microscopy (SEM) images of mild steel surfaces following 2 hours of being immersed in 3.5 wt.% NaCl in the absence and addition of HMTA. The inhibition effectiveness may be assessed by comparing the SEM images of the mixtures in the absence and addition of HMTA. Figure 11a shows the steel surface in the mixture without HMTA. Several corrosion damages are visible on the surface of the steel. The surfaces of the specimens in NaCl mixtures containing 0.01 to 0.08 M HMTA are shown in Figures 11b to e. The adsorbed HMTA coating on the metal surface may be seen in the images by looking for flat and luminous regions.

Rising the concentration of HMTA causes the percentage of surface covering to increase, eventually reaching about complete level in 0.08 M. It is confirmed by these images that the introduction of HMTA to the corrosive mixture results in the production of a homogeneous protective layer extending across the surface and may shield the steel surface against corrosion.

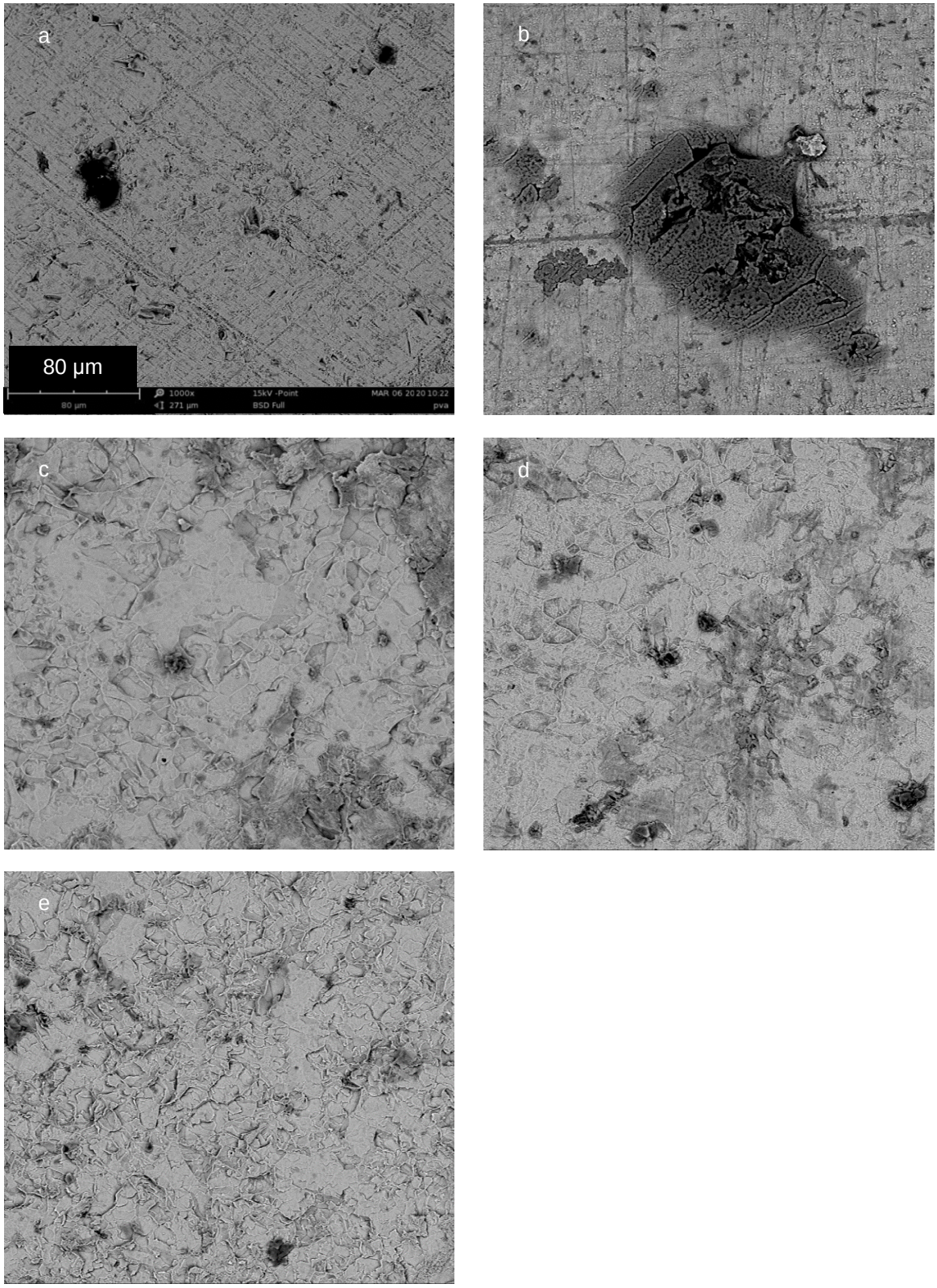

Figure 11. SEM images of mild steel surfaces backscattered by electrons (1000x) a) in the absence and presence of HMTA b) 0.01 M, c) 0.03 M, d) 0.05 M, and e) 0.08 M HMTA in 3.5 wt.% NaCl for 2 h

Slika 11. SEM slike površina od mekog čelika povratno rasejanih elektronima (1000k) a) u odsustvu i prisustvu HMTA b) 0,01 M, c) 0,03 M, d) 0,05 M, i e) 0,08 M HMTA u 3,5 tež.% NaCl za 2 h

3.6. Corrosion Inhibitor Film Characterization by EDS

The EDS (Energy Dispersive X-ray) method was used to determine the elemental structure of the steel surface following 2 hours of immersion in a 3.5 wt. % NaCl mixture. Figure 12 illustrates that the EDS range for the samples has extra unique peaks when immersed in a 3.5 wt.% NaCl mixture incorporating HMTA.

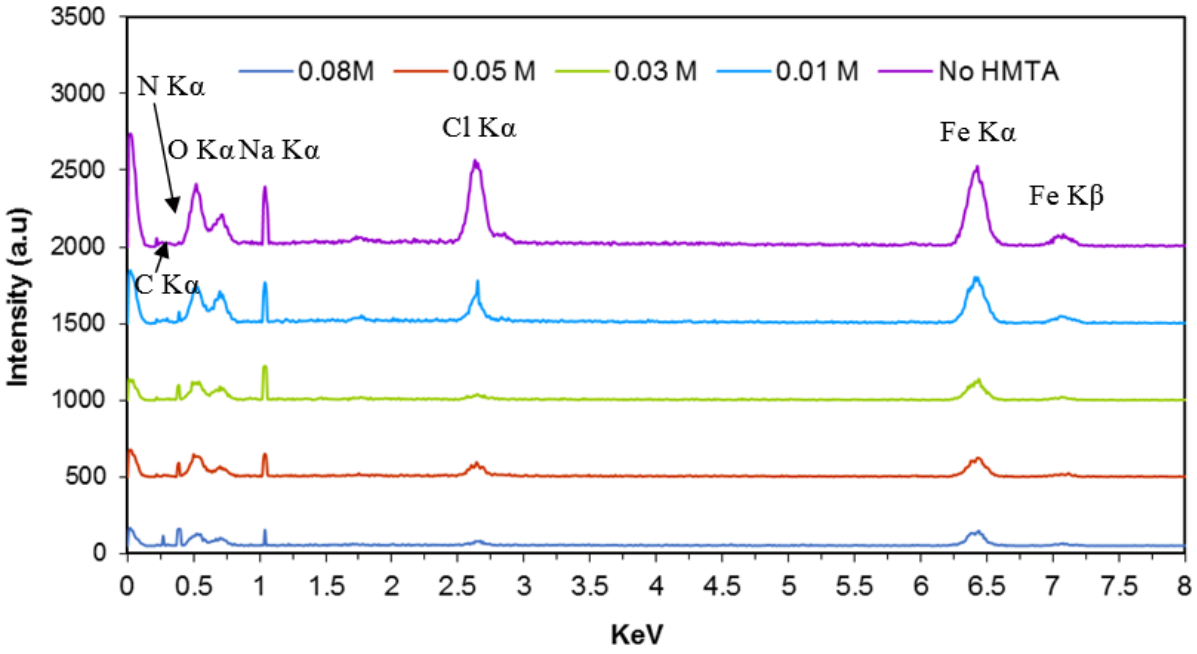

Figure 12. EDS spectrum of mild steel surfaces a) without and with b) 0.01 M, c) 0.03 M, d) 0.05 M, and e) 0.08 M HMTA in 3.5 wt.% NaCl for 2 h

Slika 12. EDS spektar površina od mekog čelika a) bez i sa b) 0,01 M, c) 0,03 M, d) 0,05 M, i e) 0,08 M HMTA u 3,5 tež.% NaCl tokom 2 h

The peaks correspond to the C and N atoms of the HMTA inhibitor (at 0.277 and 0.392 KeV, respectively), demonstrating the binding of HMTA compounds on the steel surface. Improvements in the quantity of HMTA result in a rise in the intensity of the N peak, whereas the strength of the Cl peak (at 2.622 KeV) falls concurrently.

The results showed that the deposition of HMTA compounds may delay the binding of corrosive components and that a homogeneous and flat HMTA film can reduce the abundance of surface adsorbent locations.

Mild steel's surface may include certain oxides of Fe or other components based on the presence of oxygen in the spectrum.

3.7. Surface Hardness Analysis by AFM

Following an 8-hour immersion in NaCl mixtures with and without HMTA, an AFM (Atomic Force Microscopy) topographical map of mild steel is shown in Figure 13. Regarding HMTA concentrations of 0, 0.01, 0.03, 0.05, and 0.08 M, the mean surface roughness (R_{av}) was 241, 129, 112, 97, and 56 nm, respectively. Figure 13 (a) indicates that the carbon steel displays corrosion damage and that its surface is inconsistent and rough in the mixture lacking HMTA. The sample's surface gradually gets smoother relative to the blank solution, as HMTA (0.01 to 0.05 M) is introduced to the mixtures. As seen in Figures 13(b) to 13(d), this is owing to the continuous surface covering caused by the creation of an organic film layer as a result of electrostatic reactions between surficial charged Fe atoms and bound HMTA compounds. The surface becomes smoother, as seen in Figure 13(e) when the HMTA concentration is increased to 0.08 M, which is ascribed to the steel surface's significant reduction in roughness. The homogeneous coverage of 92% is supplied by creating a film of an organic layer via the metal surface when employing 0.08 M HMTA, as shown in Figure 13(e). Creating a physical obstacle against corrosive components and reducing the chance of corrosive materials binding on potential adsorbent regions by forming a homogeneous and even film on the surface are two ways in which the organic layer protects the steel from corrosion.

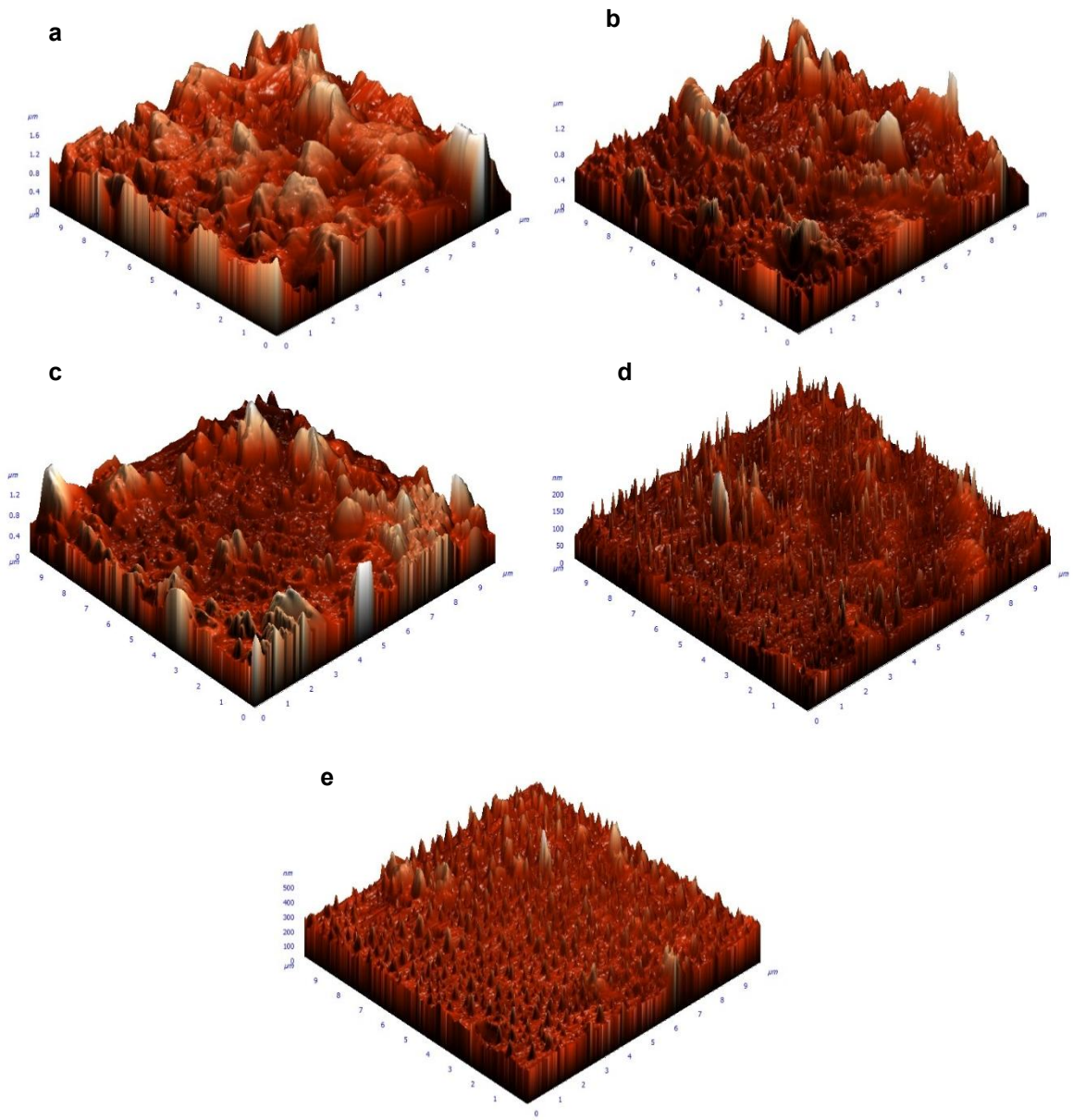

Figure 13. AFM images of mild steel following an 8-hour soaking in 3.5 wt.% NaCl containing varying concentrations of HMTA (a) 0 M, (b) 0.01 M, (c) 0.03 M, (d) 0.05 M, (e) 0.08 M.

Slika 13. AFM slike mekog čelika nakon 8-časovnog namakanja u 3,5 tež.% NaCl koji sadrži različite koncentracije HMTA (a) 0 M, (b) 0,01 M, (c) 0,03 M, (d) 0,05 M, (e) 0,08 M

3.8. Corrosion Inhibitor Film Characterization by XRD

During corrosion studies, the XRD (X-Ray Diffraction) method is usually employed to identify the primary phases or crystalline chemicals. The XRD spectrums of the mild steel specimens' surfaces following 50 minutes in a 3.5 wt.% NaCl mixture in the availability of different HMTA concentrations (0 to 0.08 M) are shown in Figure 14. In both the absence and presence of the inhibitor, the XRD spectra, and peak sites are nearly identical. Due to the adsorption of HMTA, there was no further peak. The amorphous character of biological layers is seen here. Owing to an increased HMTA quantity, the sole variation between the spectra is an elevation in peak intensities. The results of this study have shown that, rather than chemisorption of complexes through chemical interactions between Fe atoms and HMTA molecules, HMTA inhibitor is mainly adsorbed physically on the surface of the steel. There are less intense reflections from the surface

of the steel samples due to the physical adhesion of HMTA. The acquired results are consistent with the Langmuir isotherm assessment. Three peaks at 82.33°, 64.95° and 44.64° correspond to the (211), (200) and (110) planes, respectively, indicating the presence of ferrites and carbides on the carbon steel substrate [68, 69].

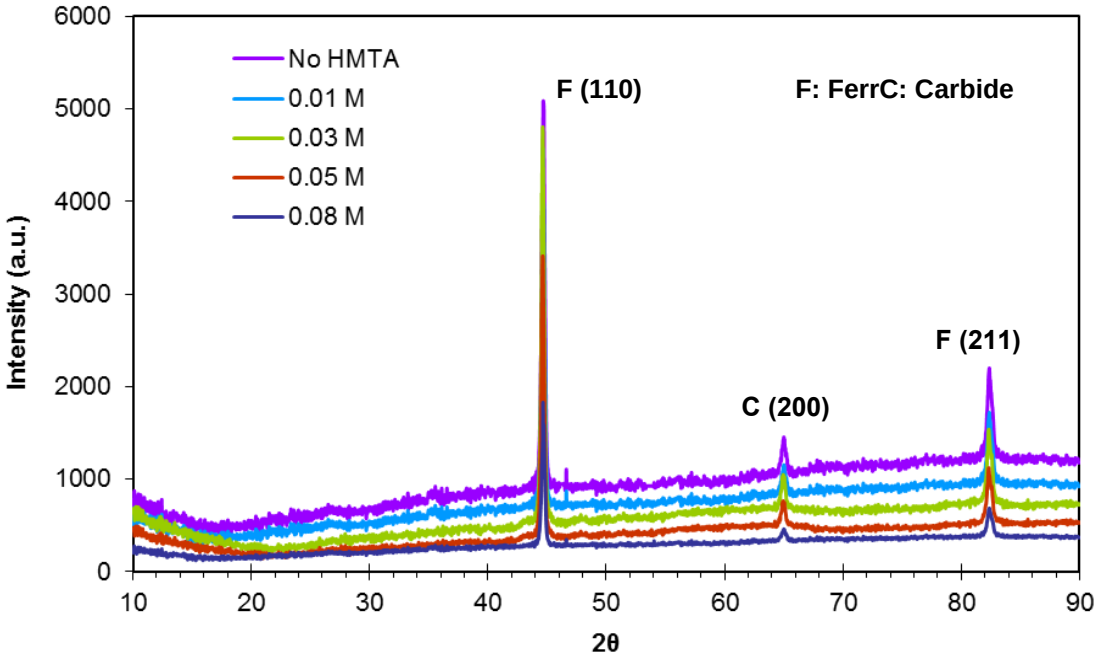

Figure 14. XRD spectra of mild steel surfaces following 2 hours of immersion in 3.5 wt.% NaCl containing varying quantities of HMTA (a) 0 M, (b) 0.01 M, (c) 0.03 M, (d) 0.05 M, (e) 0.08 M

Slika 14. XRD spektri površina od mekog čelika nakon 2 sata potapanja u 3,5 tež.% NaCl koji sadrži različite količine HMTA (a) 0 M, (b) 0,01 M, (c) 0,03 M, (d) 0,05 M, (e) 0,08 M

4. CONCLUSIONS

When used in a solution of 3.5 wt.% NaCl and 0.08 M HMTA on mild steel, HMTA's corrosion prevention efficacy is 92%. In addition, it has been shown that raising the temperature reduces the inhibitor's effectiveness. Anodic and cathodic corrosion inhibition was found to be inhibited by the Langmuir adsorption isotherm of HMTA, according to electrochemical studies. Owing to decreased corrosion current, an elevation in the HMTA concentrations leads to a shift of the OCP and polarization graphs to higher positive potentials and, as a result, a rise in corrosion resistance. Because of the physical adsorption of HMTA molecules, the metal surface is protected from corrosion by a homogenous and durable organic film. XRD and AFM findings demonstrate that increasing the quantity of HMTA enhances the covering and thickness of the amorphous protecting surface. At the same time, the generated layer hardness significantly lowers owing to the reduction in the corrosive components (Cl^-) absorptivity, as shown by EDS information.

Acknowledgments

The authors are grateful to Research Deputy of Sharif University of Technology for partial financial support.

5. REFERENCES

[1] P.Kumari (2022) plant extracts as corrosion inhibitors for aluminum alloy in NaCL Environment-recent review, J. Chil. Chem. Soc., 67(2), 5490-5495.

[2] M.Quraishi, D.S.Chauhan (2021) Drugs as Environmentally Sustainable Corrosion Inhibitors, Sustainable Corrosion Inhibitors II: Synthesis, Design, and Practical Applications, ACS Publications, p. 1-17.

[3] A.A.Al-Amiery, A.B.Mohamad, A.A.H.Kadhum, L.M. Shaker, W.N.R.W.Isahak, M.S.Takriff (2022) Experimental and theoretical study on the corrosion inhibition of mild steel by nonanedioic acid derivative in hydrochloric acid solution, Sci. Rep.,12(1), 1-21.

[4] A.Fouda, H.El-Desoky, M.Abdel-Galeil, D.Mansour (2021) Niclosamide and dichlorphenamide: New and effective corrosion inhibitors for carbon steel in 1M HCl solution, SN Appl. Sci., 3(3), 1-20.

[5] M.A.Khaled, M.A.Ismail, A.A.El-Hossiany, A.E.-A.S. Fouda (2021) Novel pyrimidine-bichalcophene derivatives as corrosion inhibitors for copper in 1 M nitric acid solution, RSC. Adv.,11(41), 25314-25333.

[6] H.Ashassi-Sorkhabi, M.Majidi, K.Seyyedi (2004) Investigation of inhibition effect of some amino acids against steel corrosion in HCl solution, Appl. Surf. Sci., 225(1-4), 176-185.

[7] H.-L.Wang, R.-B.Liu, J.Xin (2004) Inhibiting effects of some mercapto-triazole derivatives on the corrosion of mild steel in 1.0 M HCl medium, Corros. Sci., 46(10), 2455-2466.

[8] S.Zor, B.Yazıcı, M.Erbil (2005) Inhibition effects of LAB and LABS on iron corrosion in chlorine solutions at different temperatures, Corros. Sci., 47(11), 2700-2710.

[9] C.Verma, E.E.Ebenso, M.Quraishi, C.M.Hussain (2021) Recent developments in sustainable corrosion inhibitors: design, performance and industrial scale applications, Mater. Adv., 2(12), 3806-3850.

[10] K.Tebbji, A.Aouniti, M.Benkaddour, H.Oudda, I. Bouabdallah, B.Hammouti, A.Ramdani (2005) New bipyrazolic derivatives as corrosion inhibitors of steel in 1 M HCl, Prog. Org. Coat., 54(3), 170-174.

[11] Y.Abboud, A.Abourriche, T.Saffaj, M.Berrada, M. Charrouf, A.Bennamara, A.Cherqaoui, D.Takky (2006) The inhibition of mild steel corrosion in acidic medium by 2, 2′-bis (benzimidazole), Appl. Surf. Sci., 252(23), 8178-8184.

[12] A.El-Etre (2003) Inhibition of aluminum corrosion using Opuntia extract, Corros. Sci., 45(11), 2485-2495.

[13] H.Ashassi-Sorkhabi, Z.Ghasemi, D.Seifzadeh (2005) The inhibition effect of some amino acids towards the corrosion of aluminum in 1 M HCl+ 1 M H2SO4 solution, Appl. Surf. Sci., 249(1-4), 408-418.

[14] D.Liu, X.Qiu, M.Shao, J.Gao, J.Xu, Q.Liu, H.Zhou, Z.Wang (2019) Synthesis and evaluation of hexamethylenetetramine quaternary ammonium salt as corrosion inhibitor, Werkst. Korros., 70(10), 1907-1916.

[15] V.Dhayabaran, A.Rajendran, J.R.Vimala, A. Anandhakumar (2005) Hexamine as Inhibitor for the Corrosion of Mild Steel in Acid Medium, Transa. SAEST., 40(4), 134-142.

[16] M.Kumari (2017) Use of hexamine as corrosion inhibitor for carbon steel in hydrochloric acid, Int. J. Adv. Educ. Res., 2(6), 224-235.

[17] O.Fayomi, I.Akande (2019) Corrosion mitigation of aluminium in 3.65% NaCl medium using hexamine, J. Bio. Tribocorros., 5(1), 23-31.

[18] J.Hu, Y.Wang, L.Yu, Y.Zou, Y.Wang (2015) An investigation of a combined thiourea and hexamethylenetetramine as inhibitors for corrosion of N80 in 15% HCl solution: Electrochemical experiments and quantum chemical calculation, Int.l J. Corros., 15, 342-351.

[19] E.Bayol, K.Kayakırılmaz, M.Erbil (2007) The inhibitive effect of hexamethylenetetramine on the acid corrosion of steel, Mater. Chem. Phys.,104(1), 74-82.

[20] R.Vashi, D.Naik (2010) Hexamine as Corrosion Inhibitors forZinc in Phosphoric Acid, J. Chem., 7(S1), S1-S6.

[21] K.Eller, E.Henkes, R.Rossbacher, H.Höke (2000) Amines, aliphatic, Ullmann's. encycl. ind. chem.

[22] J.Liu, D.He, M.Zhang, J.Dong, C.Xu (2016) Hexamethylenetetramine as a corrosion inhibitor in hydrochloric acid solution. 10.2991/icseee-16.2016.65, November 12-13, Shenzhen, China, proceedings, Atlantis Press, Adv. Eng. Res., 63, 348-351.

[23] T.Takayanagi, N.Shimakami, M.Kurashina, H. Mizuguchi, T.Yabutani (2016) Determination of the Acid-Base Dissociation Constant of Acid-Degradable Hexamethylenetetramine by Capillary Zone Electrophoresis, Anal. Sci., 32(12),1327-1332.

[24] A.Robisson, J.Dauby, S.Grandjean, G.Benay, G. Modolo (2008) Microspheres Prepared by Internal Gelation-Understanding of HMTA and urea reactions. ATALANTE, May 19-22, Montpellier, France, p.2-12.

[25] E.P.o. Additives, P.o.S.u.i.A. Feed (2015) Scientific Opinion on the safety and efficacy of hexamethylene tetramine as a silage additive for pigs, poultry, bovines, sheep, goats, rabbits and horses, EFSA. J., 13(2), 4014-4023.

[26] A.Ogunbadejo, O.Oladele, J.Olajide, O.Obolo, S. Olusegun, P.Olubambi, S.Aribo (2018) Flow-accelerated corrosion inhibition of steel in hydrochloric acid by hexamethylenetetramine: gravimetric, density functional theory and multiphysical studies, J. Bio. Tribocorros., 4(4),1-13.

[27] S.Aribo, S.Olusegun, G.Rodrigues, A.Ogunbadejo, B.Igbaroola, A.Alo, W.Rocha, N.Mohallem, P. Olubambi (2020) Experimental and theoretical investigation on corrosion inhibition of hexamethylenetetramine [HMT] for mild steel in acidic solution, J. Taiwan. Inst. Chem.Eng., 112, 222-231.

[28] E.Mor, V.Scotto, C.Wrubl (1972) Hexamethylen-etetramine Hydroiodide (HMTA-I) as a Corrosion Inhibitor for Steel in HCl Pickling Solutions, Br. Corros. J., 7(6), 276-280.

[29] J.F.Kitchens, W.Harward, D.M.Lauter, R.Wentsel, R.S. Valentine 1978, Preliminary Problem Definition Study of 48 Munitions Related Chemicals. Volume I. Explosives Related Chemicals, ATLANTIC RESEARCH CORP ALEXANDRIA VA.

[30] (2021) ASTM G44-21: Standard Practice for Exposure of Metals and Alloys by Alternate Immersion in Neutral 3.5 % Sodium Chloride Solution.

[31] J.Suk, D.W.Kim, Y.Kang (2014) Electrodeposited 3D porous silicon/copper films with excellent stability and high rate performance for lithium-ion batteries, J. Mater. Chem. A., 2(8), 2478-2481.

[32] A.Singh, Y.Caihong, Y.Yaocheng, N.Soni, Y.Wu, Y. Lin (2019) Analyses of new electrochemical techniques to study the behavior of some corrosion mitigating polymers on N80 tubing steel, ACS. Omega., 4(2), 3420-3431.

[33] H.Wang, Electrochemical investigation of "green" film-forming corrosion inhibitors, Master Thesis, Royal Institute of Technology Stockholm, Sweden, January 2011.

[34] J.Baux, N.Caussé, J.Esvan, S.Delaunay, J.Tireau, M.Roy, D.You, N.Pébère (2018) Impedance analysis of film-forming amines for the corrosion protection of a carbon steel, Electrochim. Acta., 283 699-707.

[35] A.E.-A.S. Fouda, A.A.Nazeer, M.Ibrahim, M.Fakih (2013) Ginger extract as green corrosion inhibitor for steel in sulfide polluted salt water, J. Korean. Chem. Soc., 57(2), 272-278.

[36] M.Deyab, R.Essehli, B.El Bali (2015) Inhibition of copper corrosion in cooling seawater under flowing conditions by novel pyrophosphate, RSC. Adv., 5(79), 64326-64334.

[37] J.K.Odusote, O.M.Ajayi (2013) Corrosion inhibition of mild steel in acidic medium by jathropha curcas leaves extract, J. Electrochem. Sci. Tech., 4(2), 81-87.

[38] C.Verma, I.Obot, I.Bahadur, E.-S.M.Sherif, E.E. Ebenso (2018) Choline based ionic liquids as sustainable corrosion inhibitors on mild steel surface in acidic medium: gravimetric, electrochemical, surface morphology, DFT and Monte Carlo simulation studies, Appl. Surf. Sci., 457, 134-149.

[39] A.Popova, E.Sokolova, S.Raicheva, M.Christov (2003) AC and DC study of the temperature effect on mild steel corrosion in acid media in the presence of benzimidazole derivatives, Corros. Sci., 45(1), 33-58.

[40] V.Sivakumar, K.Velumani, S.Rameshkumar (2018) Colocid dye-a potential corrosion inhibitor for the corrosion of mild steel in acid media, Mater. Res., 21(4), 20170167.

[41] R.Solmaz, M.Mert, G.Kardaş, B.Yazici, M.Erbil (2008) Adsorption and corrosion inhibition effect of 1, 1′-thiocarbonyldiimidazole on mild steel in H2SO4 solution and synergistic effect of iodide ion, Acta. Phys-Chem. Sin., 24(7), 1185-1191.

[42] A.O.Yüce, B.D.Mert, G.Kardaş, B.Yazıcı (2014) Electrochemical and quantum chemical studies of 2-amino-4-methyl-thiazole as corrosion inhibitor for mild steel in HCl solution, Corros. Sci., 83, 310-316.

[43] H.Bentrah, Y.Rahali, A.Chala (2014) Gum Arabic as an eco-friendly inhibitor for API 5L X42 pipeline steel in HCl medium, Corros. Sci., 82, 426-431.

[44] N.Soltani, N.Tavakkoli, M.Khayatkashani, M.R. Jalali, A.Mosavizade (2012) Green approach to corrosion inhibition of 304 stainless steel in hydrochloric acid solution by the extract of Salvia officinalis leaves, Corros. Sci., 62, 122-135.

[45] M.Parveen, M.Mobin, S.Zehra, R.Aslam (2018) L-proline mixed with sodium benzoate as sustainable inhibitor for mild steel corrosion in 1M HCl: An experimental and theoretical approach, Sci. Rep., 8(1), 1-18.

[46] D.Ortega-Toledo, J.Gonzalez-Rodriguez, M. Casales, L.Martinez, A.Martinez-Villafañe (2011) CO_2 corrosion inhibition of X-120 pipeline steel by a modified imidazoline under flow conditions, Corros. Sci., 53(11), 3780-3787.

[47] E.Oguzie, Y.Li, F.Wang (2007) Corrosion inhibition and adsorption behavior of methionine on mild steel in sulfuric acid and synergistic effect of iodide ion, J. Colloid. Interface. Sci., 310(1), 90-98.

[48] A.I.Vogel (1956) Practical organic chemistry, Longmans, 2, 676-681.

[49] H.Khaleel, A.A.Ateeq, A.A.Ali (2018) The effect of temperature and inhibitor on corrosion of carbon steel in acid solution under static study, Int. J. Appl. Eng. Res., 13, 3638-3647.

[50] S.Manimegalai, P.Manjula (2015) Thermodynamic and adsorption studies for corrosion inhibition of mild steel in aqueous media by Sargasam swartzii (brown algae), J. Mater. Environ. Sci., 6(6), 1629-1637.

[51] A.K.Singh, M.Quraishi (2010) The effect of some bis-thiadiazole derivatives on the corrosion of mild steel in hydrochloric acid, Corros. Sci., 52(4), 1373-1385.

[52] N.Negm, Y.Elkholy, M.Zahran, S.Tawfik (2010) Corrosion inhibition efficiency and surface activity of benzothiazol-3-ium cationic Schiff base derivatives in hydrochloric acid, Corros.Sci., 52(10), 3523-3536.

[53] X.Li, S.Deng, G.Mu, H.Fu, F.Yang (2008) Inhibition effect of nonionic surfactant on the corrosion of cold rolled steel in hydrochloric acid, Corros. Sci., 50(2), 420-430.

[54] G.Moretti, F.Guidi, G.Grion (2004) Tryptamine as a green iron corrosion inhibitor in 0.5 M deaerated sulphuric acid, Corros. Sci., 46(2), 387-403.

[55] D.D.Do Adsorption analysis: equilibria and kinetics, Imperial college press London1998.

[56] G.K.Gomma, M.H.Wahdan (1994) Effect of temperature on the acidic dissolution of copper in the presence of amino acids, Mater. Chem. Phys., 39(2), 142-148.

[57] G.K.Gomma, M.H.Wahdan (1995) Schiff bases as corrosion inhibitors for aluminium in hydrochloric acid solution, Mater. Chem. Phys., 39(3), 209-213.

[58] F.M.Donahue, K.Nobe (1965) Theory of organic corrosion inhibitors: adsorption and linear free energy relationships, J. Electrochem. Soc.,112(9) 886-896.

[59] E.Khamis, F.Bellucci, R.Latanision, E.El-Ashry (1991) Acid corrosion inhibition of nickel by 2-(triphenosphoranylidene) succinic anhydride, Corros., 47(9), 677-686.

[60] B.Zerga, A.Attayibat, M.Sfaira, M.Taleb, B. Hammouti, M.E.Touhami, S.Radi, Z.Rais (2010) Effect of some tripodal bipyrazolic compounds on C38 steel corrosion in hydrochloric acid solution, J. Appl. Electrochem., 40(9), 1575-1582.

[61] E.A.Noor, A.H.Al-Moubaraki (2008) Thermodynamic study of metal corrosion and inhibitor adsorption processes in mild steel/1-methyl-4 [4′(-X)-styryl pyridinium iodides/hydrochloric acid systems, Mater. Chem. Phys., 110(1), 145-154.

[62] Y.Tang, F.Zhang, S.Hu, Z.Cao, Z.Wu, W.Jing (2013) Novel benzimidazole derivatives as corrosion inhibitors of mild steel in the acidic media. Part I: gravimetric, electrochemical, SEM and XPS studies, Corros. Sci., 74, 271-282.

[63] R.Solmaz, G.Kardaş, M.Çulha, B.Yazıcı, M.Erbil (2008) Investigation of adsorption and inhibitive effect of 2-mercaptothiazoline on corrosion of mild steel in hydrochloric acid media, Electrochim. Acta., 53(20), 5941-5952.

[64] A.Shahmoradi, N.Talebibahmanbigloo, A. Javidparvar, G.Bahlakeh, B.Ramezanzadeh (2020) Studying the adsorption/inhibition impact of the cellulose and lignin compounds extracted from agricultural waste on the mild steel corrosion in HCl solution, J. Mol. Liq., 304, 112751.

[65] A.A.Javidparvar, R.Naderi, B.Ramezanzadeh (2020) Manipulating graphene oxide nanocontainer with benzimidazole and cerium ions: Application in epoxy-based nanocomposite for active corrosion protection, Corros. Sci., 165, 108379.

[66] A.A.Javidparvar, R.Naderi, B.Ramezanzadeh (2020) L-cysteine reduced/functionalized graphene oxide application as a smart/control release nanocarrier of sustainable cerium ions for epoxy coating anti-corrosion properties improvement, J. Hazard. Mater., 389, 122135.

[67] R.Geethanjali, S.Subhashini (2013) Synthesis of magnetite-containing polyaniline–polyacrylamide nanocomposite, characterization and corrosion inhibition behavior on mild steel in acid media, Chem. Sci. Trans., 2(4) , 1148-1159.

[68] P.K.Sinha, M.K.Kumar, V.Kain (2015) Effect of microstructure of carbon steel on magnetite formation in simulated Hot Conditioning environment of nuclear reactors, J. Nucl. Mater., 464, 20-27.

[69] R.Crane, T.Scott (2013) The effect of vacuum annealing of magnetite and zero-valent Iron nanoparticles on the removal of aqueous uranium, J. Nanotechnol., 2013, ID 173625. https://doi.org/ 10. 1155/2013/173625

IZVOD

ISTRAŽIVANJE SVOJSTAVA INHIBICIJE KOROZIJE HEKSAMINA (HMTA) ZA MEKI ČELIK U RASTVORU NaCl

Efikasan inhibitor korozije za čelik je heksamin (HMTA). Bilo je nekoliko studija o njegovim karakteristikama inhibiranja korozije, posebno u rastvoru NaCl. Tokom ovog istraživanja ispitivane su elektrohemijske karakteristike performansi HMTA u rastvoru NaCl 3,5 tež.%. Pored toga, ispitivana su svojstva HMTA filma na površini čelika. Kada su testirani u rastvoru NaCl, elektrohemijski rezultati su otkrili da je HMTA veoma efikasan inhibitor korozije za meki čelik, sa efikasnošću od 92% u koncentraciji od 0,08 M. HMTA je pokazao aktivnost mešovitog tipa u smislu inhibicije, prema nalazima. Zbog fizičke adsorpcije HMTA jedinjenja, kao što pokazuju rezultati XRD, formiran je organski sloj kao strategija za inhibiciju HMTA. HMTA filmovi smanjuju adsorpciju hloridnih jona kao korozivnog faktora, prema EDS i termodinamičkim studijama.

Ključne reči: *heksamin (HMTA), inhibicija korozije, meki čelik, rastvor NaCl*

Naučni rad
Rad primljen: 07. 09. 2022.
Rad prihvaćen: 01. 10. 2022.
Rad je dostupan na sajtu:www.idk.org.rs/casopis